RESEARCH ARTICLE | FEBRUARY 16 2017

Enhancement of the total focusing method imaging for immersion testing of anisotropic carbon fiber composite structures FREE

Ameni Aschy; Nicolas Terrien; Sébastien Robert; Mourad Bentahar

AIP Conf. Proc. 1806, 040005 (2017)
https://doi.org/10.1063/1.4974592

Enhancement of the Total Focusing Method Imaging for Immersion Testing of Anisotropic Carbon Fiber Composite Structures

Ameni Aschy[1, a)], Nicolas Terrien[1], Sébastien Robert[2], Mourad Bentahar[3]

[1] *CETIM, Department of pressure equipment and instrumentation engineering, Nantes, France*
[2] *CEA, LIST, Department of Imaging and Simulation,* F-91191 Gif-sur-Yvette, *France*
[3] *LAUM, Acoustic Laboratory of the Maine University, UMR CNRS 6613, LE MANS Cedex 9, France*

a) Corresponding author: ameni.aschy@cetim.fr

Abstract. The use of composite structures has importantly increased because of their reduced weight, assembly simplification and excellent specific strength and stiffness. The multiple possibilities of their manufacturing allow today to integrate within a single structure multiple functions: design, mechanical strength, multi-material…These structures, by their geometric and structural complexity (anisotropy, attenuation and scattering noise), do not always allow the application of conventional ultrasound real-time methods. In this communication, the problem related to anisotropy is treated in a first part with an analysis of the influence of materials properties on the conventional array imaging methods. In the second part, anisotropy is taken into account in the Total Focusing Method (TFM) to improve the image quality in carbon fiber composite plates.

INTRODUCTION

Carbon fiber composite structures are becoming more important in the construction of aerospace structures and other industries because of their low weight and their remarkable mechanical properties. Hence, master these structures from conception, during and after their manufacturing, represents an important issue in NDE. The control and repair of these advanced materials require an in-depth knowledge of composite structures and a reliable detection of defects. This study is brought up with simulations and experiments in an immersion testing configuration for carbon fiber composite structures with different types of symmetry (orthotropic, transverse isotropic…). Firstly, a comparison of different real-time methods is conducted to highlight the influence of the material on the capabilities of the different imaging techniques. Secondly, defects are imaged with the TFM [1] associated with a ray-based model that takes into account the directional dependence of ultrasonic velocity in an anisotropic carbon fiber composite in order to correct the image quality.

EVALUATION OF CONVENTIONAL REAL TIME METHODS

Principle of the Imaging Methods and Experimental Set-up

We begin with an evaluation of conventional real-time methods with a carbon epoxy aerospace standard featuring artificial defects distributed in three parts of different thicknesses (see Fig. 1). The goal is to evaluate these methods in terms of sensitivity of detection, signal-to-noise ratio (SNR) and inspection speed in order to favor the use of a specific method over another. This comparison is done between two methods based on linear scan [2]: focused line-

43rd Annual Review of Progress in Quantitative Nondestructive Evaluation, Volume 36
AIP Conf. Proc. 1806, 040005-1–040005-8; doi: 10.1063/1.4974592
Published by AIP Publishing. 978-0-7354-1474-7/$30.00

scan and focused line-scan with Dynamic Depth Focusing (DDF) and three methods based on incident plane waves: Single Plane Wave Imaging (SPWI); SPWI with sums in receive mode, and focused SPWI with delays and sums in receive mode.

SPWI is a fast imaging method consisting in the transmission of a single plane wave by firing all the elements, and receiving elementary signals in parallel [3]. The ideal number of receivers in the sub-arrays that provides the best SNR was determined with the help of simulations performed with the CIVA software platform.

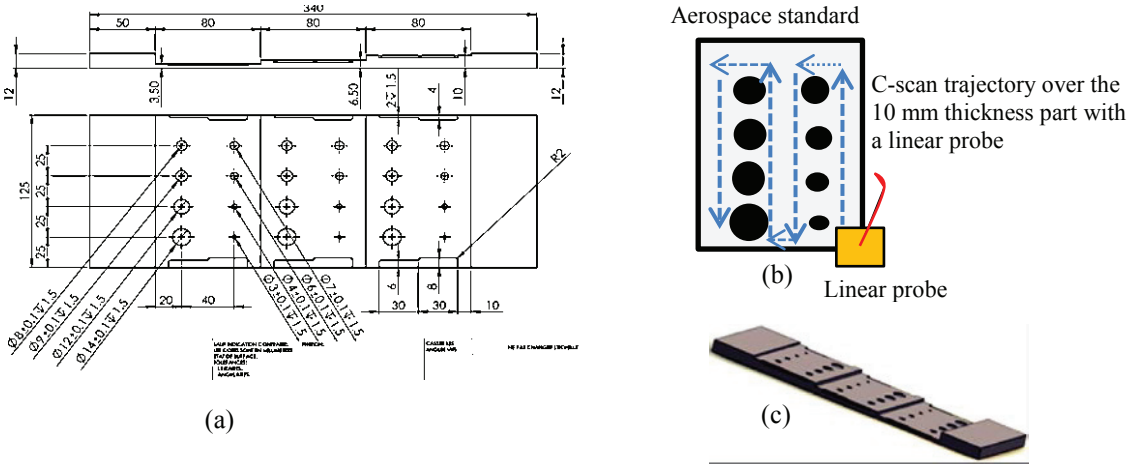

FIGURE 1. Aerospace standard carbon epoxy including artificial defects: (a) Drawing definition; (b) C-scan trajectory over the part of 10 mm thickness; (c) 3D view.

Results and Discussion

Acquisitions were made in immersion to inspect the 10 mm thickness area (see figure 1(b)) with a linear transducer (64 elements, 5 MHz center frequency, 0.6 mm pitch).The Cscan obtained with the different methods are displayed in Fig. 2.

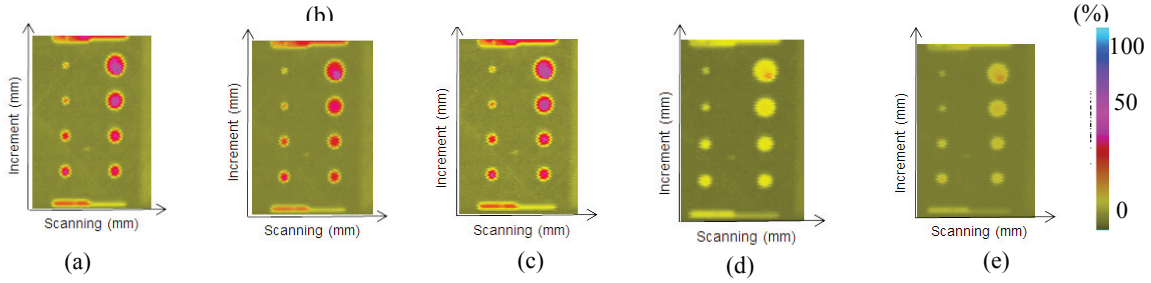

FIGURE 2. Cscan images obtained by: (a) focused line scan with DDF; (b) focused line scan; (c) focused SPWI ;(d) SPWI with multiple sums in receive mode ;(e) SPWI.

Results revealed that focused SPWI, focused line scan and focused line scan with DDF offer the best SNRs (see Fig. 3(a)), and a greater accuracy in the defect characterization (measurement of the echo widths at half-height) (see Fig. 3 (b)). Focused SPWI gives the fastest inspection speed with a maximum acquisition frequency equal to 1413 Hz, while the scanning speed is reduced to 262 Hz for the focused line scan associated with DDF and 292 Hz for the focused line scan (see Table 1).

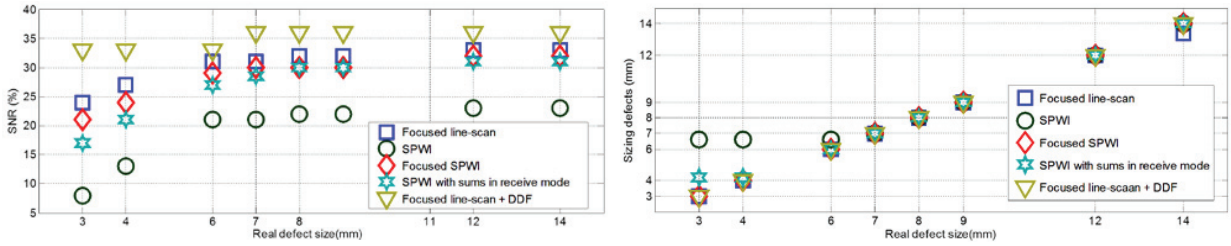

(a) (b)

FIGURE 3. Evolution of (a) SNR and (b) sizing defect for the 5 imaging methods.

Focused SPWI offers the best compromise between the speed inspection, the SNR and the sizing of defects. In addition, it can be observed that focusing in receive mode for SPWI increases the SNR by nearly 10 %.

TABLE 1. Maximum of the inspection speed.

Increase in the scanning speed ↓	**Conventional real-time methods**	**Maximum acquisition frequency (Hz)**
	Focused line-scan + DDF	262
	Focused line-scan	292
	SPWI	1149
	SPWI (with sums in receive)	1225
	Focused SPWI(with delays and sums in receive)	1413

In SPWI, a plane wave is transmitted at normal incidence in the composite plate, and a L0 focusing is performed for the two focused line scan methods. This is the reason why these imaging techniques are not significantly affected by the structural anisotropy. When the composite is slightly heterogeneous, some noise would disrupt the images resolution. Thus, in the next section, we will try to improve the quality of images (limitation of shadowing effects, improvement the spatial resolution) by applying focusing algorithms which allows better defects discrimination. TFM allows focusing in all directions, but the variation of phase velocities according to the direction of propagation is not considered in current TFM. In the following, TFM will be enhanced by considering the anisotropic stiffness properties of the carbon fiber composite structures.

TFM IMPROVEMENTS FOR ANISOTROPIC COMPOSITE STRUCTURES

Theoretical Background

First, we perform the data acquisition called Full Matrix Capture (FMC) [4] that consists in recording the set of the $N \times N$ inter-element impulse signals $k_{pq}(t)$ of a linear probe with N elements, where $k_{pq}(t)$ is the signal received by element q when transmitting with element p.

Usually, TFM [1] for isotropic media focuses in both transmit and receive modes the set of $N \times N$ analytic signals $s_{pq}(t) = k_{pq}(t) + jH[k_{pq}(t)]$ at every point of a region of interest (H denotes the Hilbert's transform) considering a constant velocity in the imaging equation. The "anisotropic TFM" use the Christoffel equation to determinate the phase velocity and the polarization of ultrasonic waves [5]. Quasi-longitudinal wave slowness curve in an anisotropic material were calculated and used in the TFM algorithm in order to take into account the velocity variation according the focusing direction (see Fig. 4).

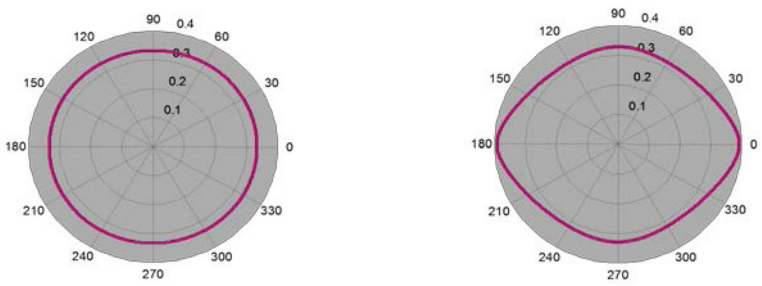

(a) (b)

FIGURE 4. Wave slowness curves (a) Longitudinal waves in an isotropic materials (b) Quasi-longitudinal waves in an anisotropic materials.

The TFM imaging equation for anisotropic materials can be written as:

$$A(\vec{\mathbf{r}}, \theta_{Cijkl}) = \left|\sum_{p=1}^{N}\sum_{q=p}^{N}(2-\delta_{pq})\mu_p(\vec{\mathbf{r}}, \theta_{Cijkl})v_q(\vec{\mathbf{r}}, \theta_{Cijkl})s_{pq}[t_{pq}(\vec{\mathbf{r}}, \theta_{Cijkl})]\right| \quad (1)$$

where $\vec{\mathbf{r}}$ is the position vector of a focusing point $M(x,z)$ and θ_{Cijkl} is the phase angle with the symmetry axis of the wave propagation. δ_{pq} is the Kronecker's symbol ($\delta_{pq}=1$ if $p=q$, $\delta_{pq}=0$ otherwise) introduced to take into account the reciprocity principle in the image calculation, i.e. $k_{pq}(t) = k_{qp}(t)$. This reduces the number of sums from $N \times N$ *to* $N \times (N+1)/2$ at every focusing point. $\mu_p(\vec{\mathbf{r}}, \theta_{Cijkl})$ and $v_q(\vec{\mathbf{r}}, \theta_{Cijkl})$ are apodisation or weighting factors, in transmission and reception respectively, introduced to filter imaging artifacts (due to aliasing effects, aperture edge diffraction effects, geometry echoes, attenuation in anisotropic media…).

When a transducer array is immersed in water above a specimen with plate surface described by $Z = H_0$(see Figure 5), with H_0 is the water level, the inter-element propagation time from a transmitter p to a receiver q can be expressed as follows:

$$t_{pq}\left(\overrightarrow{\boldsymbol{r}}, \theta_{Cijkl}\right) = \frac{\|\vec{r}_p^S - \vec{r}_p\|}{c_1} + \frac{\|\vec{r} - \vec{r}_p^S\|}{c_2(\theta_{Cijkl})} + \frac{\|\vec{r}_q^S - \vec{r}_q\|}{c_1} + \frac{\|\vec{r} - \vec{r}_q^S\|}{c_2(\theta_{Cijkl})} \quad (2)$$

where t_p^{tr} and t_q^{re} are the theoretical times of flight associated with incident and backscattered waves, respectively. In the following, only quasi-longitudinal waves are considered in TFM imaging, without taking into account mode conversions. Thus, t_p^{tr} is equal to t_q^{re} for p = q and the problem can be reduced to the calculation of the forward propagation time t_p^{tr} from a transmitter p to the focusing point M. With the notations introduced in Figure 5, it can be expressed as:

$$t_p^{tr}\left(\overrightarrow{\boldsymbol{r}}, \theta_{Cijkl}\right) = \frac{\|\vec{r}_p^S - \vec{r}_p\|}{c_1} + \frac{\|\vec{r} - \vec{r}_p^S\|}{c_2(\theta_{Cijkl})} \quad (3)$$

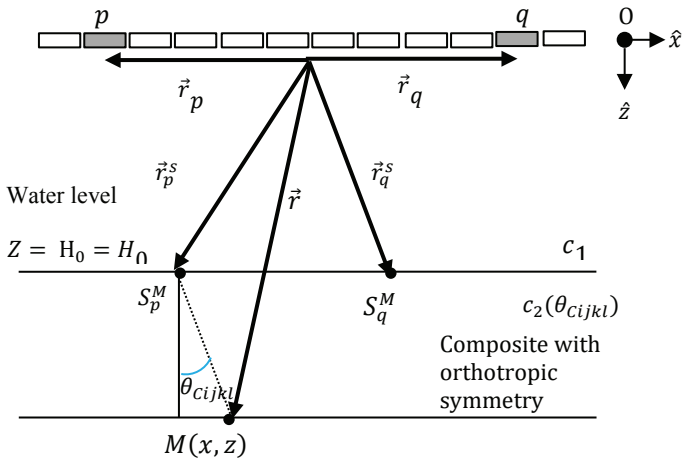

FIGURE 5. 2D imaging geometry used for the TFM formulation: immersion array above a plate water/solid interface.

c_1 and $c_2(\theta_{Cijkl})$ are the wave velocities in water and in carbon fiber composite. $\overrightarrow{\mathbf{r_p^s}}$ (resp.$\overrightarrow{\mathbf{r_q^s}}$) is the position vector of the intersection point S_p^M (resp. S_q^M) between the surface H_0 and the ultrasonic ray coming from transmitter p (resp. q) to the focusing point $M(x,z)$.

In this part, we seek to determine the abscissa of the intersection point S_p^M and according to the Fermat's principle, the wave propagation through the water/solid interface has to correspond to the minimum propagation time. Therefore, by developing the Euclidean norms in Eq. (3) the Fermat's principle leads to the determination of the surface point (abscissa X) that minimizes the function t_p^{tr}:

$$t_p^{tr}(X) = f_p(X) = \frac{1}{c_1}\sqrt{(X - x_p)^2 + {H_0}^2} + \frac{1}{c_{2(\theta_{Cijkl})}}\sqrt{(X - x)^2 + [H_0 - z]^2} \tag{4}$$

In the context of embedded processing in portable systems, one of the most efficient algorithms in terms of simplicity and robustness is the gradient descent method:

$$\begin{cases} X^{(k+1)} = X^{(k)} - \frac{{f'}_p(X^{(k)})}{{f''}_p(X^{(k)})} \\ \theta_{Cijkl} = arctan\left(\frac{X^{(k)} - x}{H_0 - z}\right) \end{cases} \tag{5}$$

where $\overrightarrow{\boldsymbol{r}} = (x; z)$,$\overrightarrow{\boldsymbol{r_p^s}} = (X; H_0)$, $\overrightarrow{\boldsymbol{r_p}} = (x_p; 0)$, X_p is the intersection point between the surface H_0 and the ultrasonic ray coming from the transmitter p, the exponent *'(k)' (*$k \in \mathbb{N}$) denotes the iteration step. $f_p'(X)$ and $f_p''(X)$ are the first and second derivatives *of* $f_p(X)$ with respect to X. They are numerically computed with finite differences to accelerate processing times.

The impact point S_p^M is situated between the transmitter and the focusing point. In addition, the velocity in water being lower than the ones in the inspected medium, the impact point is located closer to the emitter abscissa x_p. In this case the starting value $X^{(0)}$is set equal to the element abscissa *(*$X^{(0)} = x_p$*)*. Once the impact point coordinates are known, the distance between the element and the focusing point can be calculated geometrically thus giving the corresponding propagation time (see Eq.3). Finally for every transmitter/receiver pair and every point in the region of interest, the amplitudes associated to the computed times of flight are added following Eq. 1, to form the TFM image.

Results and Discussion

Effect of Anisotropy on the TFM Imaging

The anisotropy effects in imaging have been studied with simulated data. A linear array probe (64 elements, 5MHz center frequency) is used in immersion to image a carbon fiber specimen (20mm thickness) with orthotropic symmetry with 9 independent elastic components. The composite plate contains several side drilled holes (with 0.5mm diameter) at different depths (figure 6). The time of flight t_p^{tr} with for p= 64 is calculated for both symmetry types (isotropic and orthotropic symmetries) and for all the focusing points *M(x, z)*.

At this level, the anisotropy effects on the TFM images are studied by considering an isotropic homogeneous medium in the wave propagation model equivalent to the orthotropic one.

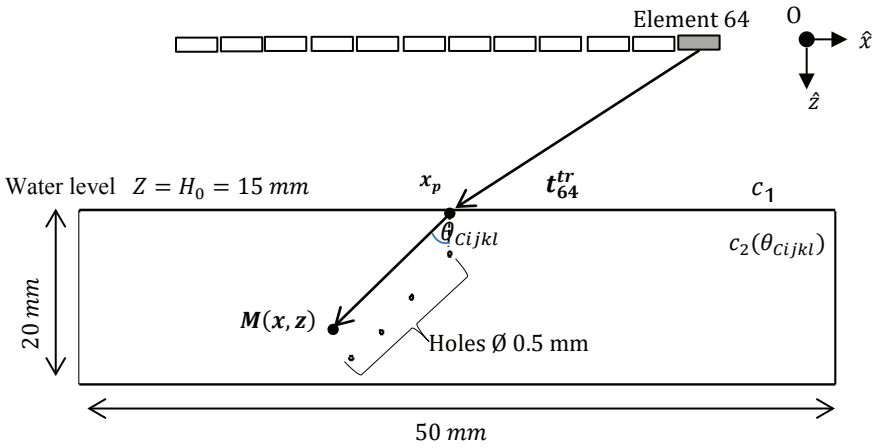

FIGURE 6. Ray path from a transmitter to a focusing point M passing through the water/solid interface

The time of flight expressed in µs for the isotropic medium (figure 7(a)) seems to be the same as the time of flight for the anisotropic medium (figure 7(b)).

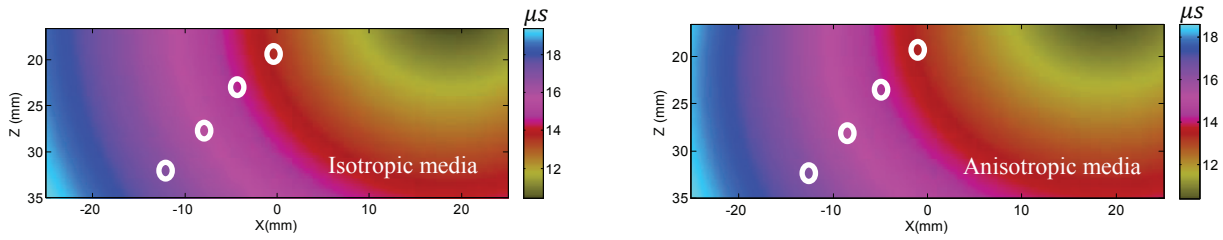

FIGURE 7. Map of times of flight expressed in µs for (a) the isotropic (b) and the anisotropic media

In figure 8, the difference of times of flight Δt can be expressed in rad. ($\Delta\phi = 2\pi f \Delta t$) in order to better quantify the impact of the anisotropy in imaging. The phases difference between both media shows a strong error around the defect location when the last element of the probe is used as transmitter.

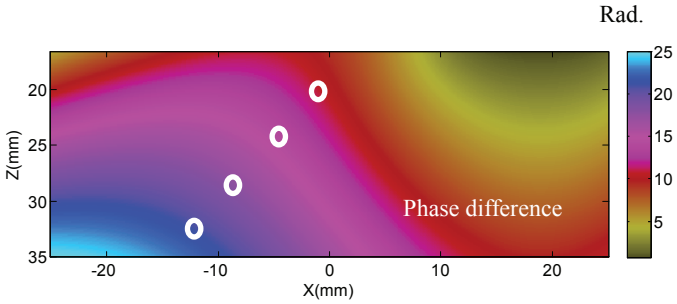

FIGURE 8. Difference of times of flight expressed in rad: strongest errors are located around the series of defects.

In figure 9 below, the images are calculated by processing signals simulated in isotropic (Fig. 9(a)) and anisotropic plates (figure 9 (b)) with the same inspection configuration described in Fig. 6. In the second case, the TFM algorithm is applied to the data assuming an isotropic medium, which means that the times of flight calculated with the ray-based model are not in agreement with the wave propagation times in the medium. In isotropic media, TFM gives the optimal spatial resolution at every point (figure 9, (a)) but in the orthotropic media, echoes are altered because of the anisotropy of the material (figure 9, (b)). This explains the necessity to take into account the anisotropy in the time of flight calculation model.

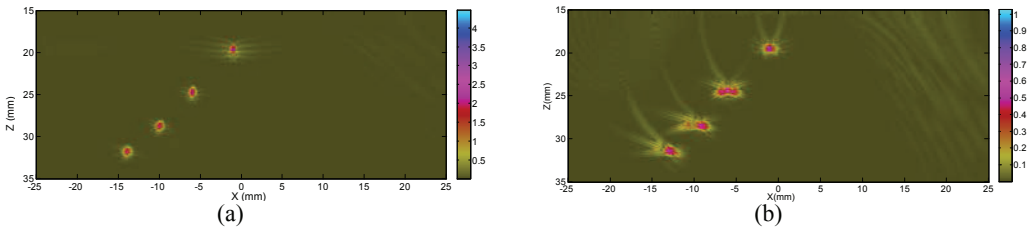

FIGURE 9. TFM images: (a) in an isotropic plate; (b) in an anisotropic plate assuming isotropic wave propagation for the time-of-flight calculation (b).

The Enhancement of TFM for Anisotropic Media

Considering the profile of quasi- longitudinal waves and their propagation direction in an anisotropic carbon fiber material with orthotropic symmetry, the TFM equation (Eq. (1)) now provides an optimal spatial resolution at all the points of the region of interest (figure 10).

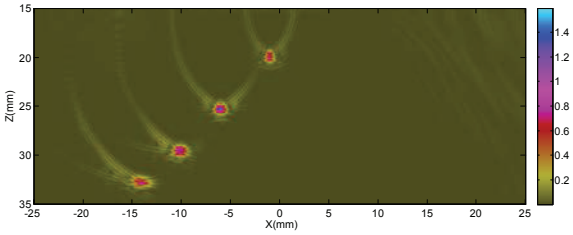

FIGURE 10. Image obtained by taking into account the anisotropic wave propagation in the plate.

CONCLUSIONS AND PERSPECTIVES

In this communication, a comparison of conventional real-time ultrasonic methods has been done to inspect a flat carbon fiber structure to determinate the advantages and the limitations of each method in order the favor the use of one to another. Then, the influence of material properties on TFM images has been evaluated and has shown that "isotropic" TFM method does not take into account the anisotropic stiffness of composite structures which deteriorate the image quality. Therefore, TFM has been enhanced to be extended to anisotropic structures.

The evaluation and validation of enhanced TFM will be pursued in case of plane surfaces by considering the attenuation of the quasi-longitudinal waves, as a function of the incident angle, in different anisotropic media in order to correct the defect location errors on one hand, and to reduce the scattering noise on the other hand. In case of convincing results, this work will be extended to complex surfaces and to Plane Wave Imaging (PWI) [6] method for composites structures.

REFERENCES

1. M. Karaman, P.C. Li, "Synthetic aperture imaging for small scale systems", IEEE Transactions on Ultrasonics Ferroelectrics and Frequency Control **42**, 429–442 (1995).
2. S. Mahaut, C. Gondard, "Ultrasonic defect characterization with a dynamic adaptive focusing system", Proceedings of Ultrasonics International, **34**(2–5), 121–124 (1996).
   P. David Shattuck, D. Marc Weinshenker, "Explososcan: a parallel processing technique for high speed ultrasound imaging with linear phased arrays", J Acoust Soc Am., **75**(4), 1273-1282 (1984).
3. M. Weston, P. Mudge, "Time efficient auto-focusing algorithms for ultrasonic inspection of dual-layered media using Full Matrix Capture", NDT&E International, **47**, 43–50 (2012).
4. D. Royer, E. Dieulesaint, "Ondes élastiques dans les solides", Vol. 1, Masson, (1996).
5. L. Lejeune,S. Robert, "Plane Wave Imaging for ultrasonic non-destructive testing: Generalization to multimodal imaging", Ultrasonics, **64**, 128–138 (2016).